Title	Insulator-semiconductor interface fixed charges in AlGaN/GaN metal-insulator-semiconductor devices with Al_20_3 or AlTiO gate dielectrics
Author(s)	Le, Son Phuong; Nguyen, Duong Dai; Suzuki,Toshi-kazu
Citation	Journal of Applied Physics, 123(3): 034504-1-034504-7
Issue Date	2018-01-19
Type	Journal Article
Text version	publisher
URL	http://hdl.handle.net/10119/15737
Rights	Copyright 2018 American Institute of Physics. This article may be downloaded for personal use only. Any other use requires prior permission of the author and the American Institute of Physics. The following article appeared in Son Phuong Le, Duong Dai Nguyen, and Toshi-kazu Suzuki, Journal of Applied Physics, 123(3), 034504 (2018) and may be found at http://dx.doi.org/10.1063/1.5017668
Description	

JOURNAL OF APPLIED PHYSICS **123**, 034504 (2018)

Insulator-semiconductor interface fixed charges in AlGaN/GaN metal-insulator-semiconductor devices with Al_2O_3 or AlTiO gate dielectrics

Son Phuong Le, Duong Dai Nguyen, and Toshi-kazu Suzuki[a)]
Center for Nano Materials and Technology, Japan Advanced Institute of Science and Technology (JAIST), 1-1 Asahidai, Nomi, Ishikawa 923-1292, Japan

(Received 29 November 2017; accepted 3 January 2018; published online 19 January 2018)

We have investigated insulator-semiconductor interface fixed charges in AlGaN/GaN metal-insulator-semiconductor (MIS) devices with Al_2O_3 or AlTiO (an alloy of Al_2O_3 and TiO_2) gate dielectrics obtained by atomic layer deposition on AlGaN. Analyzing insulator-thickness dependences of threshold voltages for the MIS devices, we evaluated positive interface fixed charges, whose density at the AlTiO/AlGaN interface is significantly lower than that at the Al_2O_3/AlGaN interface. This and a higher dielectric constant of AlTiO lead to rather shallower threshold voltages for the AlTiO gate dielectric than for Al_2O_3. The lower interface fixed charge density also leads to the fact that the two-dimensional electron concentration is a decreasing function of the insulator thickness for AlTiO, whereas being an increasing function for Al_2O_3. Moreover, we discuss the relationship between the interface fixed charges and interface states. From the conductance method, it is shown that the interface state densities are very similar at the Al_2O_3/AlGaN and AlTiO/AlGaN interfaces. Therefore, we consider that the lower AlTiO/AlGaN interface fixed charge density is not owing to electrons trapped at deep interface states compensating the positive fixed charges and can be attributed to a lower density of oxygen-related interface donors. *Published by AIP Publishing.* https://doi.org/10.1063/1.5017668

I. INTRODUCTION

GaN-based heterojunction field-effect transistors (HFETs)[1] are important devices owing to their high current drive capability and high breakdown voltages. However, there are several disadvantages of GaN-based HFETs; self-heating effects,[2–4] current collapse phenomena,[5,6] and also gate leakage currents are limiting factors for the practical use of these devices. For the suppression of gate leakage currents and the current collapse phenomena in GaN-based devices, it can be effective to employ metal-insulator-semiconductor (MIS) structures, which are also significant to normally off operations,[7] even though GaN-based MIS devices sometimes exhibit unstable characteristics.[8–12] As a gate dielectric of GaN-based MIS devices, high-dielectric-constant (high-k) insulators, such as Al_2O_3,[13] HfO_2,[14,15] TaON,[16] AlN,[17–21] BN,[22,23] and AlTiO,[24] have been investigated. In GaN-based MIS device processing, when an insulator is deposited on a negatively polarized III-N semiconductor surface, such as Ga-face (Al)GaN, positive insulator-semiconductor interface fixed charges tend to be generated and to cancel the negative polarization charges.[25–32] However, the existence of the insulator-semiconductor interface fixed charges is not a necessity.[29,30] Since the interface fixed charges have significant impacts on threshold voltages V_{th}, we expect that V_{th} can be controlled by "interface charge engineering,"[29] i.e., by controlling the interface fixed charges. In particular, if the positive interface fixed charge density is sufficiently suppressed, a normally off operation can be expected.[33,34] However, despite many reports on the interface fixed charges, their sufficient control is a remaining issue. Moreover, their origin is not fully elucidated even though they are attributed to positively ionized oxygen donors in some cases. Therefore, further investigations on insulator-semiconductor interface fixed charges for GaN-based MIS devices are very necessary and important towards V_{th} control and normally off operations.

In this work, we investigated insulator-semiconductor interface fixed charges in AlGaN/GaN MIS devices with Al_2O_3 or AlTiO (an alloy of Al_2O_3 and TiO_2[35–37]) gate dielectrics, which are deposited on an AlGaN/GaN heterostructure by atomic layer deposition (ALD). AlTiO has, depending on its composition, intermediate physical properties between Al_2O_3 ($k \sim 9$ and $E_g \sim 7$ eV) and TiO_2 ($k \sim 60$ and $E_g \sim 3$ eV),[37] being useful to balance the trade-off between k and energy gap E_g. Previously, we fabricated AlTiO/AlGaN/GaN MIS devices with excellent characteristics, indicating that AlTiO can be an important candidate for a gate dielectric of GaN-based MIS devices.[24] The present work involves a comparative study on insulator-semiconductor interface fixed charges in Al_2O_3/AlGaN/GaN and AlTiO/AlGaN/GaN MIS devices. By analyzing linear insulator-thickness dependences of V_{th}, we evaluated insulator-semiconductor interface fixed charges. As a result, we find that the fixed charge density at the AlTiO/AlGaN interface is significantly lower than that at the Al_2O_3/AlGaN interface. In addition, we also discuss the relationship between the interface fixed charges and interface states. It is suggested that the lower AlTiO/AlGaN interface fixed charge density is not owing to electrons trapped at deep interface states.

[a)]Author to whom correspondence should be addressed: tosikazu@jaist.ac.jp

II. DEVICE FABRICATION

Using an $Al_{0.27}Ga_{0.73}N$(30 nm)/GaN(3000 nm) heterostructure grown by metal-organic vapor phase epitaxy on sapphire(0001), we fabricated AlGaN/GaN MIS devices with Al_2O_3 or AlTiO gate dielectrics. The device fabrication was started with Ti/Al/Ti/Au Ohmic electrode formation. After surface treatments using organic solvents, oxygen plasma ashing, and an ammonium-based solution, insulator films of Al_2O_3 or AlTiO as gate dielectrics with several thicknesses $d_{ins} = 6$–29 nm were deposited on the AlGaN surface by ALD. The Al_2O_3 films ($k \sim 9$ and $E_g \sim 7$ eV) were obtained by using trimethylaluminum (TMA) and H_2O as precursors, and the Al_xTi_yO films (x:$y = 0.73$:0.27, $k \sim 13$–14, and $E_g \sim 6$ eV) were by using TMA, tetrakis-dimethylamino titanium (TDMAT), and H_2O. After post-deposition annealing in H_2-mixed Ar at 350 °C, Ni/Au gate electrode formation completed the device fabrication. As a result, we obtained Al_2O_3/AlGaN/GaN and AlTiO/AlGaN/GaN MIS devices, whose cross sections are schematically shown in Fig. 1(a), with 70 μm × 70 μm gate electrodes surrounded by the Ohmic electrodes as shown by top-view optical images in Fig. 1(b).

III. INSULATOR-SEMICONDUCTOR INTERFACE FIXED CHARGES

In order to investigate insulator-semiconductor interface fixed charges, we examined threshold voltages V_{th} of the Al_2O_3/AlGaN/GaN and AlTiO/AlGaN/GaN MIS devices, by measuring capacitance-voltage (C–V) characteristics between the gate and the grounded Ohmic electrodes. Since GaN-based MIS devices sometimes exhibit unstable V_{th} depending on the sweeping range of the gate voltage V_G,[8–12] we checked V_{th} stability; starting from $V_{G0} \geq 0$, C–V characteristics were measured under $V_G = V_{G0} \rightarrow -15$ V with a sweep rate of 0.36 V/s. Figure 2 shows an example of the measurement results for $d_{ins} = 19$ nm, at 1 MHz frequency with $V_{G0} = 0$, 1, 2, 3, 4, and 5 V. Although we find rather stable V_{th}, weak V_{th} shifts take place after positive bias applications, probably owing to charging effects of trapped electrons. Thus, to determine V_{th}, we employ $V_{G0} = 0$ V to avoid the charging effects. Figure 3(a) shows C–V characteristics of the MIS devices with $d_{ins} = 6$–29 nm, measured at 1 MHz under $V_G = 0 \rightarrow -15$ V with a sweep rate of 0.36 V/s. As shown in Fig. 3(b), the sheet concentration of the two-dimensional electron gas (2DEG) under the gate, n_s, can be obtained by integrating C as a function of V_G, from which we can determine V_{th}.

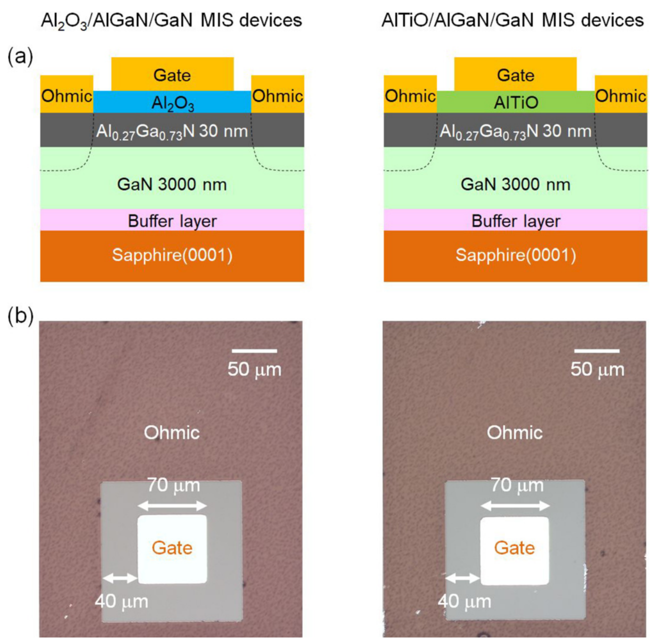

FIG. 1. (a) Schematic cross sections and (b) top-view optical images of the fabricated Al_2O_3/AlGaN/GaN and AlTiO/AlGaN/GaN MIS devices.

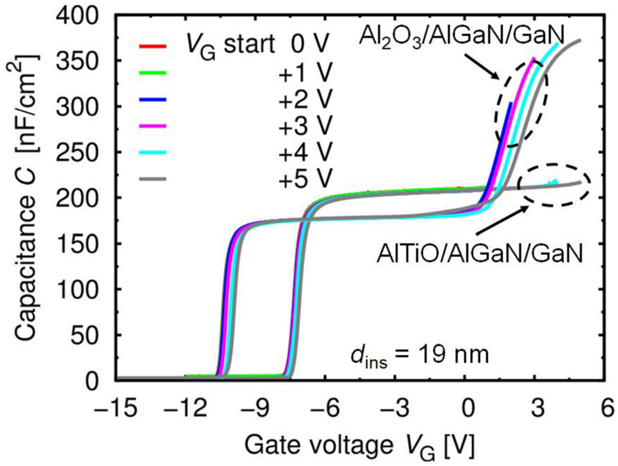

FIG. 2. Checking V_{th} stability of the Al_2O_3/AlGaN/GaN and AlTiO/AlGaN/GaN MIS devices with $d_{ins} = 19$ nm: C–V characteristics measured at 1 MHz under $V_G = V_{G0} \rightarrow -15$ V with a sweep rate of 0.36 V/s, where $V_{G0} = 0$, 1, 2, 3, 4, and 5 V.

Figure 4 shows the band diagram of AlGaN/GaN MIS devices, considering the interface fixed charges. From this, we obtain

$$\frac{\Delta\sigma_{ins} - qn_s}{k_{ins}\varepsilon_0} d_{ins} + \frac{\Delta\sigma_{AlGaN} - qn_s}{k_{AlGaN}\varepsilon_0} d_{AlGaN} = -V_G + \psi/q + E_F/q \quad (1)$$

using the elementary charge $q > 0$, the vacuum permittivity ε_0, the insulator-semiconductor interface fixed charge density σ_{ins}, the polarization charge densities σ_{GaN} and σ_{AlGaN}, the dielectric constants k_{ins} and k_{AlGaN}, the thicknesses d_{ins} and d_{AlGaN}, the 2DEG Fermi energy E_F, and $\psi = \phi - \varphi - \Delta E_C$ defined in Fig. 4, where $\Delta\sigma_{ins} = \sigma_{ins} - \sigma_{GaN}$ and $\Delta\sigma_{AlGaN} = \sigma_{AlGaN} - \sigma_{GaN}$. For $V_G = V_{th}$ ($n_s = 0$ and $E_F = 0$), we find

$$V_{th} = -\frac{\Delta\sigma_{ins}}{k_{ins}\varepsilon_0} d_{ins} - \frac{\Delta\sigma_{AlGaN}}{k_{AlGaN}\varepsilon_0} d_{AlGaN} + \psi/q \quad (2)$$

giving a linear d_{ins}-dependence of V_{th} with a slope of $-\Delta\sigma_{ins}/(k_{ins}\varepsilon_0)$. The 2DEG concentration n_s under the gate is approximately given by

$$qn_s \simeq C_0(V_G - V_{th}) \quad (3)$$

as experimentally confirmed in Fig. 3(b), where

$$\frac{1}{C_0} = \frac{d_{ins}}{k_{ins}\varepsilon_0} + \frac{d_{AlGaN}}{k_{AlGaN}\varepsilon_0}. \quad (4)$$

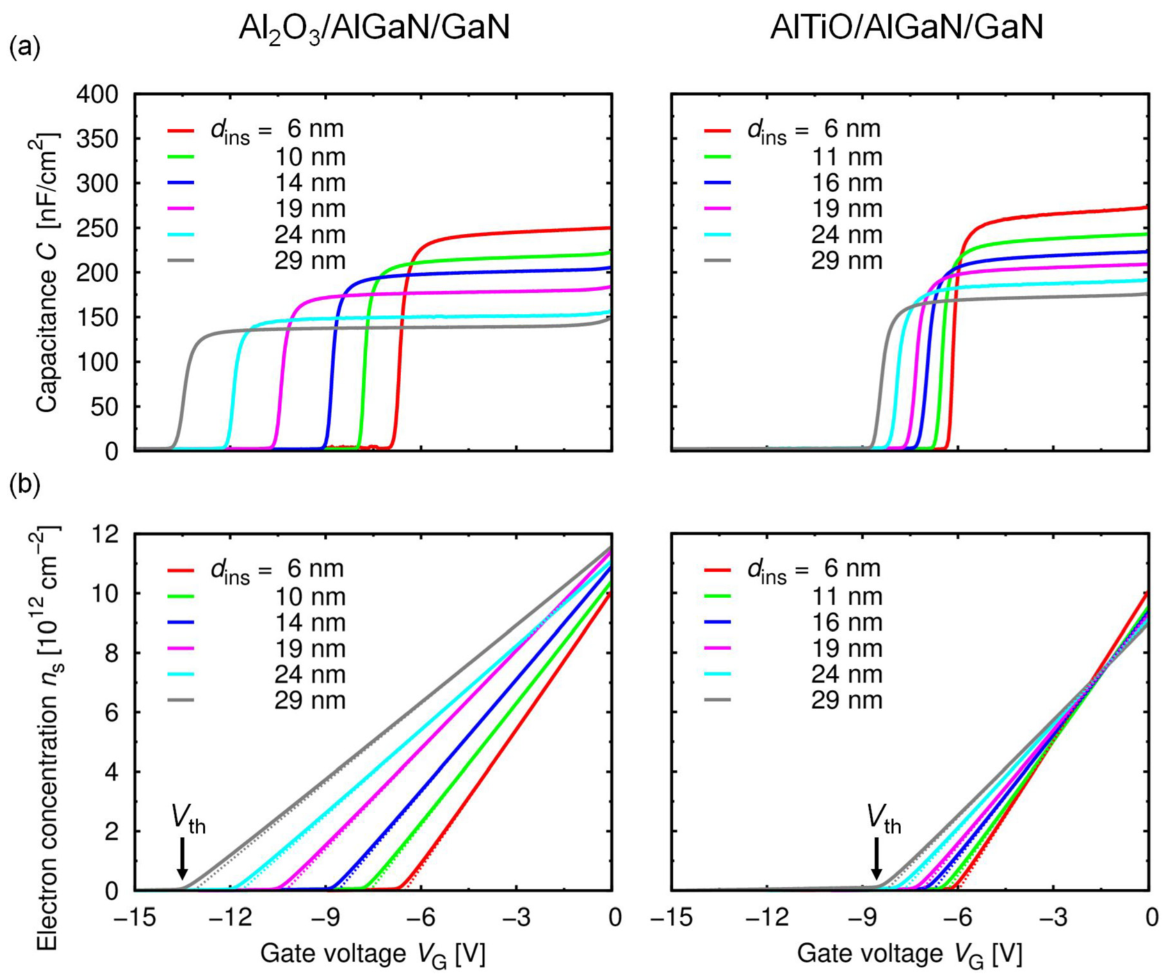

FIG. 3. (a) C–V characteristics of the Al_2O_3/AlGaN/GaN and AlTiO/AlGaN/GaN MIS devices with $d_{ins} = 6$–29 nm, measured at 1 MHz under $V_G = 0 \to -15$ V with a sweep rate of 0.36 V/s. (b) The 2DEG sheet concentration n_s obtained by integrating C as functions of the gate voltage V_G, from which we can determine V_{th}.

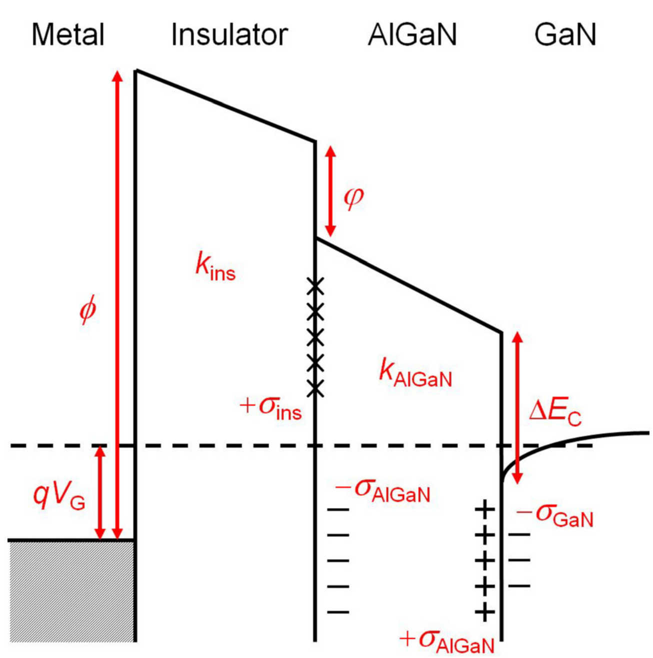

FIG. 4. The band diagram of AlGaN/GaN MIS devices, considering the interface fixed charges.

For $V_G = 0$, $n_s = n_{s0}$ is given by

$$qn_{s0} \simeq -C_0 V_{th} = \frac{\Delta\sigma_{ins} d_{ins}/(k_{ins}\varepsilon_0) + \Delta\sigma_{AlGaN} d_{AlGaN}/(k_{AlGaN}\varepsilon_0) - \psi/q}{d_{ins}/(k_{ins}\varepsilon_0) + d_{AlGaN}/(k_{AlGaN}\varepsilon_0)} \quad (5)$$

which is a nonlinear function of d_{ins}.

According to Eq. (4), $1/C_0$ is a linear function of d_{ins}. Experimentally, C_0 is estimated by C at $V_G = 0$ V as plotted in Fig. 5(a), where we can confirm the linear relation. From the slopes, we obtain dielectric constants $k_{ins} = 9.4$ and 13.4 for Al_2O_3 and AlTiO, respectively, being consistent with separated experimental results using metal-insulator-metal structures (not shown). From the intercept, we obtain $k_{AlGaN} = 9.5$ (using $d_{AlGaN} = 30$ nm). Figure 5(b) shows the experimentally determined V_{th} as functions of d_{ins}. We find linear dependences obeying Eq. (2), indicating that the interface fixed charges dominate V_{th} and also rather shallower V_{th} for AlTiO than for Al_2O_3. By fitting using Eq. (2), we obtain $\Delta\sigma_{ins}/q = 1.5 \times 10^{13}$ cm^{-2} and 7.3×10^{12} cm^{-2} at the Al_2O_3/AlGaN and AlTiO/AlGaN interfaces, respectively. The latter gives a significantly lower σ_{ins} than the former, which may be attributed to a lower-density of oxygen donors[25,31,32] at

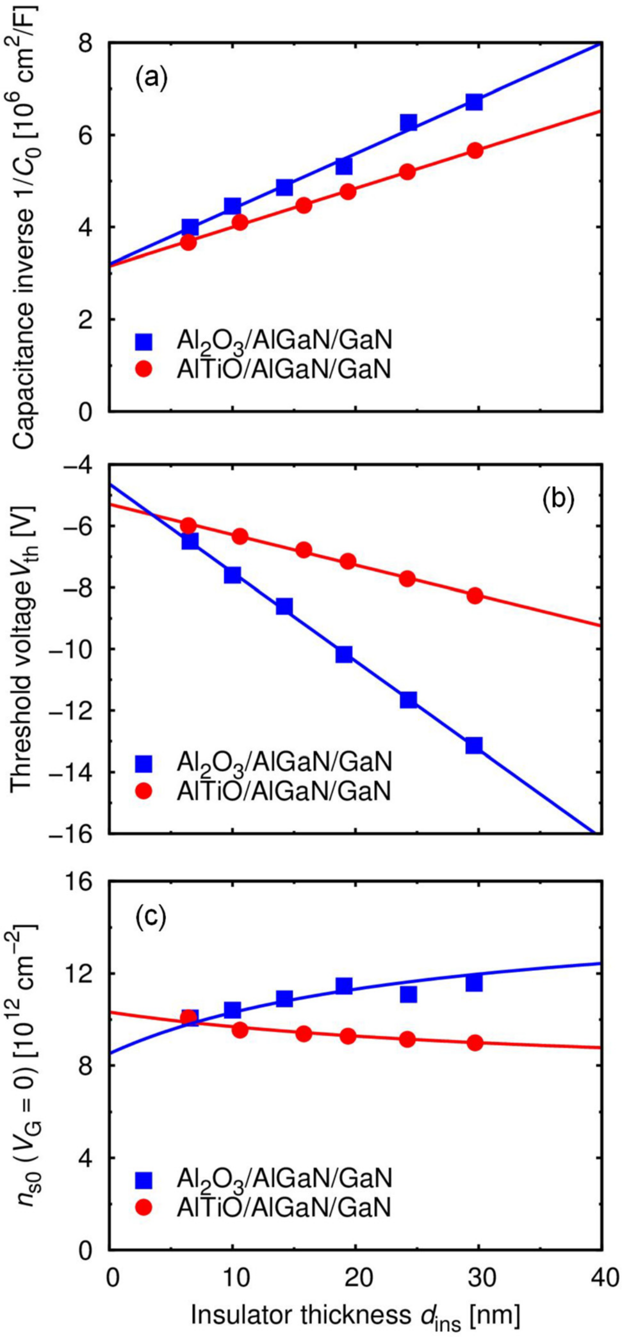

FIG. 5. (a) $1/C_0$, (b) V_{th}, and (c) n_{s0} at $V_G = 0$ of the Al_2O_3/AlGaN/GaN and AlTiO/AlGaN/GaN MIS devices, as functions d_{ins} with fitting curves.

the AlTiO/AlGaN interface. This lower σ_{ins} and the higher k_{ins} of AlTiO lead to rather shallower V_{th}. Figure 5(c) shows the experimentally obtained n_{s0} as functions of d_{ins}, whose non-linear dependences are fitted by Eq. (5). We find that n_{s0} is a decreasing function of d_{ins} for AlTiO, whereas being an increasing function for Al_2O_3. From Eq. (5), we obtain

$$\frac{\partial n_{s0}}{\partial d_{ins}} = \frac{C_0}{k_{ins}\varepsilon_0}(\Delta\sigma_{ins}/q - n_{s0}) \tag{6}$$

which implies that $\Delta\sigma_{ins}/q > n_{s0}$ leads to increasing n_{s0} with d_{ins}, while $\Delta\sigma_{ins}/q < n_{s0}$ leads to decreasing n_{s0}. Thus, for Al_2O_3 and AlTiO, n_{s0} is an increasing and a decreasing function of d_{ins}, respectively. It should be noted that, in the limit of a large d_{ins}, n_{s0} in Eq. (5) approaches to $\Delta\sigma_{ins}/q$, indicating that a normally off operation can be expected for sufficiently suppressed interface fixed charges, satisfying $\Delta\sigma_{ins} < 0$, i.e., $\sigma_{ins} < \sigma_{GaN}$. However, in the both cases, we observe $\Delta\sigma_{ins} > 0$, i.e., $\sigma_{ins} > \sigma_{GaN}$.

Even though $\Delta\sigma_{ins}$ is obtained experimentally, in order to evaluate σ_{ins}, it is necessary to assume σ_{GaN}. Hereafter, we assume $\sigma_{GaN}/q = 2.1 \times 10^{13}\,cm^{-2}$ obtained by a theoretical calculation.[38] This leads to $\sigma_{ins}/q = 3.6 \times 10^{13}\,cm^{-2}$ and $2.8 \times 10^{13}\,cm^{-2}$ at the Al_2O_3/AlGaN and AlTiO/AlGaN interfaces, respectively. In addition, these values should be compared with σ_{AlGaN}/q. Although $\Delta\sigma_{AlGaN}/q = 1.5 \times 10^{13}\,cm^{-2}$ for $Al_{0.27}Ga_{0.73}N$/GaN is obtained theoretically,[39] several experiments show lower $\Delta\sigma_{AlGaN}$, about 85% of the theoretical one.[40–42] Thus, we assume $\Delta\sigma_{AlGaN}/q = 1.3 \times 10^{13}\,cm^{-2}$, i.e., $\sigma_{AlGaN}/q = 3.4 \times 10^{13}\,cm^{-2}$. Based on the assumptions, we summarize σ_{ins} compared with σ_{AlGaN} in Fig. 6, where the dotted line corresponds to neutral insulator-semiconductor interfaces, i.e., $\sigma_{ins} + (-\sigma_{AlGaN}) = 0$. We obtain that the Al_2O_3/AlGaN interface is nearly neutral,[25] while the AlTiO/AlGaN interface is rather negatively charged owing to the lower σ_{ins}. By fitting V_{th} as functions of d_{ins} with Eq. (2), we also obtain $\psi = 2.0$ and 1.3 eV for the Al_2O_3/AlGaN/GaN and AlTiO/AlGaN/GaN MIS devices, respectively. From these, we obtain band diagrams of the AlGaN/GaN MIS devices by Poisson-Schrödinger calculation[43] as shown in Fig. 7, where we can confirm that the AlTiO/AlGaN interface is negatively charged. The directions of the electric fields in Al_2O_3 and AlTiO at $V_G = 0\,V$ are opposite, leading to the fact that n_{s0} is a decreasing function of d_{ins} for AlTiO, whereas being an increasing function for Al_2O_3.

IV. RELATION WITH INSULATOR-SEMICONDUCTOR INTERFACE STATES

It should be noted that electrons trapped at deep interface states with very long time constants can act as (quasi) negative interface fixed charges.[30] Therefore, the interface fixed charge measurements might be influenced by electrons at deep interface states compensating the positive fixed

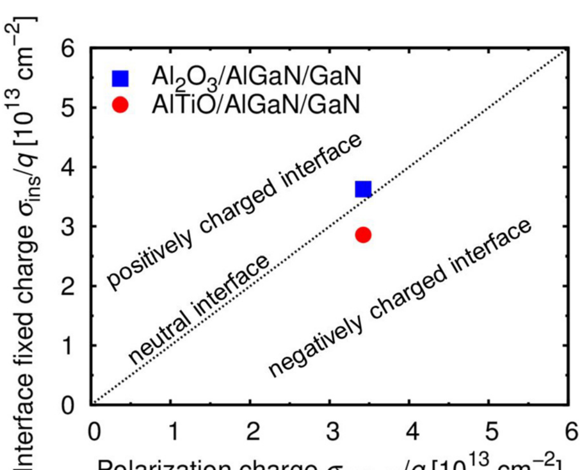

FIG. 6. A comparison between the insulator-semiconductor interface fixed charge density σ_{ins} and AlGaN polarization charge density σ_{AlGaN}.

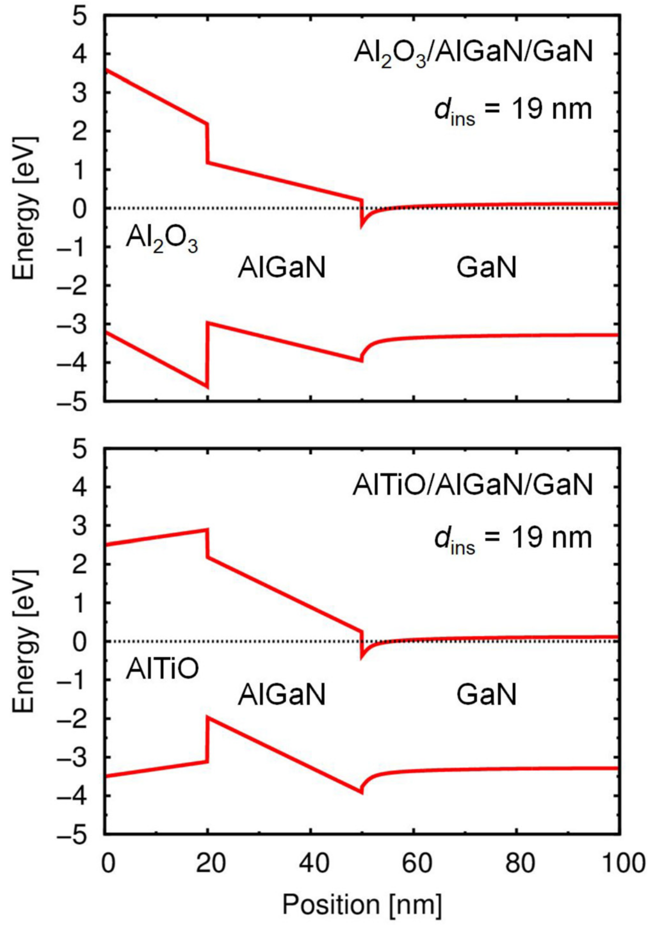

FIG. 7. Band diagrams of the Al_2O_3/AlGaN/GaN and AlTiO/AlGaN/GaN MIS devices at $V_G = 0$ V, obtained by 1D Poisson-Schrödinger calculation.

charges. In particular, there is a possibility that the lower AlTiO/AlGaN interface fixed charge density is owing to electrons trapped at deep interface states. In order to consider this possibility, we examined the interface states at Al_2O_3/AlGaN and AlTiO/AlGaN by frequency dependent *C–V* measurements. Figure 8 shows examples of the measurement results, *C–V* characteristics at 100 Hz–1 MHz for the Al_2O_3/AlGaN/GaN and AlTiO/AlGaN/GaN MIS devices with $d_{ins} = 14$–19 nm. In any cases, no frequency dispersion is observed for negative bias voltages, showing that the V_{th} determination is not affected by the measurement frequency. On the other hand, for positive bias voltages, frequency dispersions are observed, suggesting insulator-semiconductor interface states.

The conductance method[44] was applied to the frequency dependent *C–V* characteristics to evaluate the interface state density.[30,45–51] Assuming the equivalent circuit shown in the insets of Fig. 9, which consists of an interface state capacitance C_i, an interface state conductance G_i, and an AlGaN capacitance C_{AlGaN} in parallel, with an insulator capacitance C_{ins} connected in series, we obtained the frequency dependence of G_i for the Al_2O_3/AlGaN/GaN and AlTiO/AlGaN/GaN MIS devices. Figure 9 shows examples of obtained G_i/ω as functions of frequency *f*, where $\omega = 2\pi f$, exhibiting single-peaked behavior. As shown by the curves in Fig. 9, the single-peaked behavior is well fitted by[52]

$$\frac{G_i}{\omega} = \frac{q^2 D_i \ln(1 + \omega^2\tau^2)}{2\omega\tau}, \tag{7}$$

where D_i is the interface state density and τ is the trapping time constant, giving the peak frequency $f_p = 1/(\pi\tau)$ and the peak value of $G_i/\omega \simeq 0.4 q^2 D_i$. The observed peaks are summarized in Fig. 10(a), where we find very similar behavior

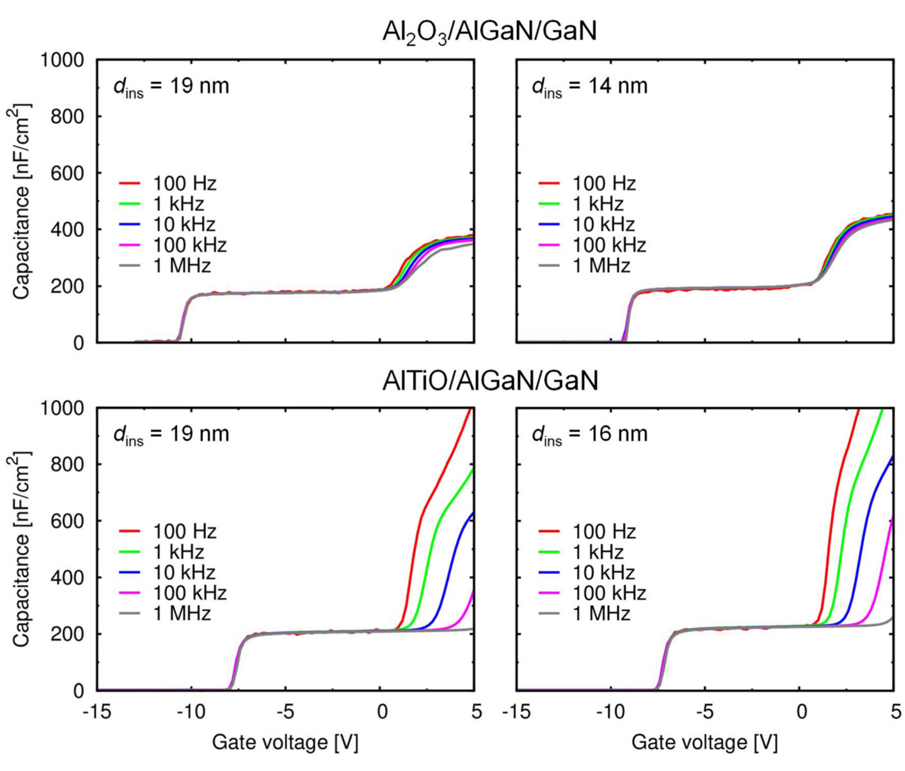

FIG. 8. *C–V* characteristics of the Al_2O_3/AlGaN/GaN and AlTiO/AlGaN/GaN MIS devices with $d_{ins} = 14$–19 nm, measured at 100 Hz–1 MHz.

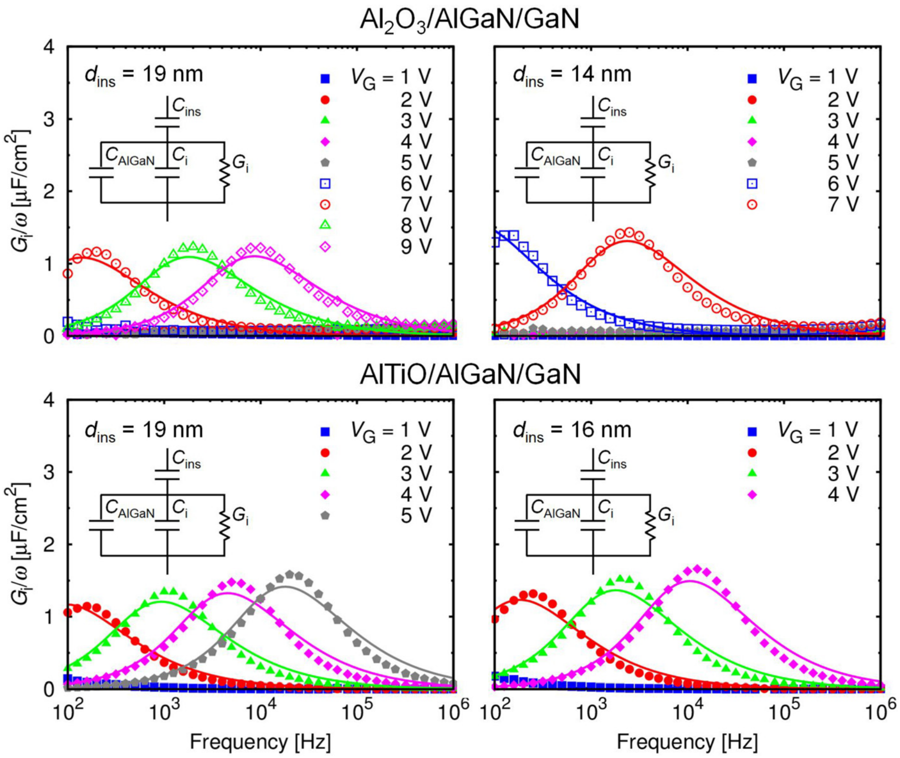

FIG. 9. G_i/ω as functions of frequency with fitting curves for the Al_2O_3/AlGaN/GaN and AlTiO/AlGaN/GaN MIS devices. Insets: The small-signal equivalent circuit.

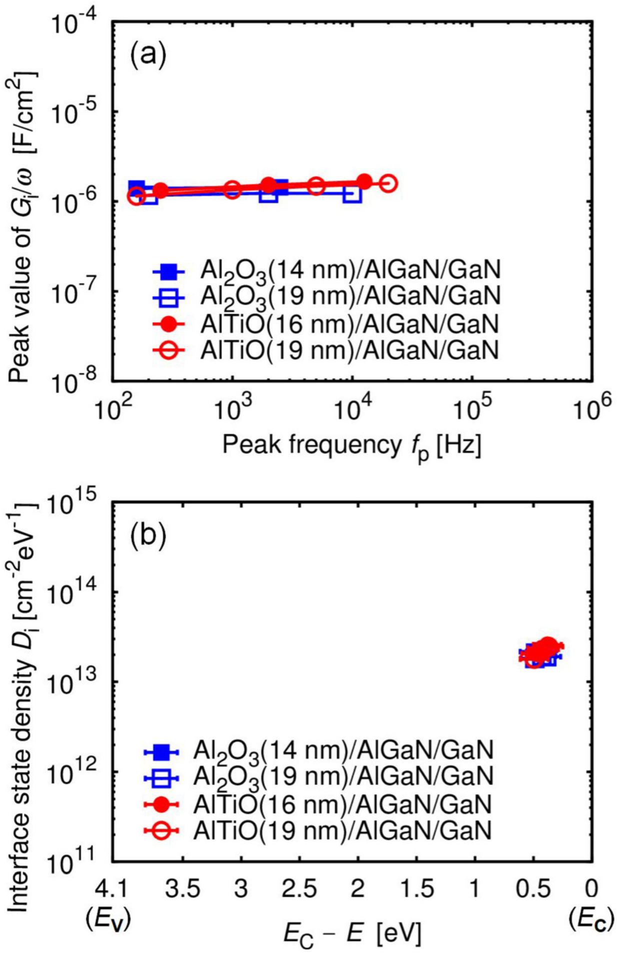

FIG. 10. (a) The peak value of G_i/ω as functions of peak frequency f_p and (b) the interface state density D_i as functions of the energy $(E_C - E)$, for the Al_2O_3/AlGaN/GaN and AlTiO/AlGaN/GaN MIS devices.

for Al_2O_3/AlGaN/GaN and AlTiO/AlGaN/GaN and also for different d_{ins}, suggesting that the behavior is dominated by interface states with very similar densities at Al_2O_3/AlGaN and AlTiO/AlGaN. From the peaks, we can obtain the relationship between D_i and τ. Moreover, τ for an interface state at the energy E is given by $\tau = \tau_0 \exp[(E_C - E)/k_B T]$ using the Boltzmann constant k_B, temperature T, and the conduction band bottom energy E_C, where τ_0 is a time constant determined by the capture cross section of the trap. Thus, using τ_0, we can estimate the relationship between D_i and $(E_C - E)$. Even though τ_0 is ambiguous, assuming a wide range of $\tau_0 = 1$–100 ps, we show D_i as functions of $(E_C - E)$ in Fig. 10(b), where the error bars correspond to the wide range of τ_0 values. This indicates a very similar shallow interface state density $D_i \sim 2 \times 10^{13}\,cm^{-2}eV^{-1}$ of Al_2O_3/AlGaN and AlTiO/AlGaN and suggests that deep interface state densities are also similar, even though the interface fixed charge density σ_{ins} is rather lower at AlTiO/AlGaN. Thus, we should conclude that there is no correlation between the interface fixed charges and the interface states in our case, as reported in Ref. 32. This suggests that the lower σ_{ins} at AlTiO/AlGaN is not owing to electrons trapped at deep interface states, compensating the positive fixed charges. Since interface states generally have a U-shaped density of states, from the shallow interface state density above, we can expect a deep interface state density of $\lesssim 10^{13}\,cm^{-2}eV^{-1}$ or less. On the other hand, the difference between σ_{ins}/q at Al_2O_3/AlGaN and that at AlTiO/AlGaN is $\sim 0.8 \times 10^{13}\,cm^{-2}$. Thus, it is not plausible that the difference is due to trapped electrons at the deep interface states. Although the material origin of the lower σ_{ins} at AlTiO/AlGaN is not clear, it is possible to tentatively assume a lower density of oxygen-related interface donors, where strong Ti-O bonding may suppress donor formation.

V. CONCLUSION

We have investigated insulator-semiconductor interface fixed charges in Al_2O_3/AlGaN/GaN and AlTiO/AlGaN/GaN MIS devices. The AlTiO/AlGaN interface gives significantly lower-density interface fixed charges and rather shallower threshold voltages. The lower interface fixed charge density also leads to the fact that the 2DEG concentration is a decreasing function of the AlTiO thickness, whereas being an increasing function of the Al_2O_3 thickness. Moreover, we discuss the relationship between the interface fixed charges and interface states. Since the interface state densities are very similar at Al_2O_3/AlGaN and AlTiO/AlGaN, it is suggested that the lower interface fixed charge density at AlTiO/AlGaN is not owing to electrons trapped at deep interface states, compensating the positive fixed charges. Thus, a lower density of oxygen-related donors at the AlTiO/AlGaN interface can be assumed, where strong Ti-O bonding may suppress donor formation. We consider that the results can provide a clue towards V_{th} control and normally off operations of GaN-based MIS devices.

ACKNOWLEDGMENTS

This work was supported by JSPS KAKENHI Grant Nos. 26249046 and 15K13348.

[1]M. Khan, A. Bhattarai, J. Kuznia, and D. Olson, Appl. Phys. Lett. **63**, 1214 (1993).
[2]R. Gaska, A. Osinsky, J. Yang, and M. Shur, IEEE Electron Device Lett. **19**, 89 (1998).
[3]M. Kuball, J. Hayes, M. Uren, I. Martin, J. Birbeck, R. Balmer, and B. Hughes, IEEE Electron Device Lett. **23**, 7 (2002).
[4]X. D. Wang, W. D. Hu, X. S. Chen, and W. Lu, IEEE Trans. Electron Devices **59**, 1393 (2012).
[5]R. Vetury, N. Zhang, S. Keller, and U. Mishra, IEEE Trans. Electron Devices **48**, 560 (2001).
[6]G. Meneghesso, G. Verzellesi, R. Pierobon, F. Rampazzo, A. Chini, U. K. Mishra, C. Canali, and E. Zanoni, IEEE Trans. Electron Devices **51**, 1554 (2004).
[7]T. Oka and T. Nozawa, IEEE Electron Device Lett. **29**, 668 (2008).
[8]Y. Lu, S. Yang, Q. Jiang, Z. Tang, B. Li, and K. J. Chen, Phys. Status Solidi C **10**, 1397 (2013).
[9]M. Ťapajna, M. Jurkovič, L. Válik, Š. Haščík, D. Gregušová, F. Brunner, E.-M. Cho, and J. Kuzmík, Appl. Phys. Lett. **102**, 243509 (2013).
[10]P. Lagger, M. Reiner, D. Pogany, and C. Ostermaier, IEEE Trans. Electron Devices **61**, 1022 (2014).
[11]T.-L. Wu, D. Marcon, B. Bakeroot, B. D. Jaeger, H. C. Lin, J. Franco, S. Stoffels, M. V. Hove, R. Roelofs, G. Groeseneken, and S. Decoutere, Appl. Phys. Lett. **107**, 093507 (2015).
[12]K. Nishiguchi, S. Kaneki, S. Ozaki, and T. Hashizume, Jpn. J. Appl. Phys., Part 1 **56**, 101001 (2017).
[13]T. Hashizume, S. Ootomo, and H. Hasegawa, Appl. Phys. Lett. **83**, 2952 (2003).
[14]C. Liu, E. F. Chor, and L. S. Tan, Appl. Phys. Lett. **88**, 173504 (2006).
[15]A. Kawano, S. Kishimoto, Y. Ohno, K. Maezawa, T. Mizutani, H. Ueno, T. Ueda, and T. Tanaka, Phys. Status Solidi C **4**, 2700 (2007).
[16]T. Sato, J. Okayasu, M. Takikawa, and T. Suzuki, IEEE Electron Device Lett. **34**, 375 (2013).
[17]Y. Liu, J. Bardwell, S. McAlister, S. Rolfe, H. Tang, and J. Webb, Phys. Status Solidi C **0**, 69 (2003).
[18]H.-A. Shih, M. Kudo, M. Akabori, and T. Suzuki, Jpn. J. Appl. Phys., Part 1 **51**, 02BF01 (2012).
[19]H.-A. Shih, M. Kudo, and T. Suzuki, Appl. Phys. Lett. **101**, 043501 (2012).
[20]H.-A. Shih, M. Kudo, and T. Suzuki, J. Appl. Phys. **116**, 184507 (2014).
[21]S. P. Le, T. Q. Nguyen, H.-A. Shih, M. Kudo, and T. Suzuki, J. Appl. Phys. **116**, 054510 (2014).
[22]J.-C. Gerbedoen, A. Soltani, M. Mattalah, M. Moreau, P. Thevenin, and J.-C. D. Jaeger, Diamond Relat. Mater. **18**, 1039 (2009).
[23]T. Q. Nguyen, H.-A. Shih, M. Kudo, and T. Suzuki, Phys. Status Solidi C **10**, 1401 (2013).
[24]S. P. Le, T. Ui, T. Q. Nguyen, H.-A. Shih, and T. Suzuki, J. Appl. Phys. **119**, 204503 (2016).
[25]S. Ganguly, J. Verma, G. Li, T. Zimmermann, H. Xing, and D. Jena, Appl. Phys. Lett. **99**, 193504 (2011).
[26]M. Esposto, S. Krishnamoorthy, D. N. Nath, S. Bajaj, T.-H. Hung, and S. Rajan, Appl. Phys. Lett. **99**, 133503 (2011).
[27]M. Ťapajna and J. Kuzmík, Appl. Phys. Lett. **100**, 113509 (2012).
[28]J. Son, V. Chobpattana, B. M. McSkimming, and S. Stemmer, Appl. Phys. Lett. **101**, 102905 (2012).
[29]T.-H. Hung, S. Krishnamoorthy, M. Esposto, D. N. Nath, P. S. Park, and S. Rajan, Appl. Phys. Lett. **102**, 072105 (2013).
[30]M. Ťapajna, M. Jurkovič, L. Válik, Š. Haščík, D. Gregušová, F. Brunner, E.-M. Cho, T. Hashizume, and J. Kuzmík, J. Appl. Phys. **116**, 104501 (2014).
[31]M. Matys, B. Adamowicz, A. Domanowska, A. Michalewicz, R. Stoklas, M. Akazawa, Z. Yatabe, and T. Hashizume, J. Appl. Phys. **120**, 225305 (2016).
[32]M. Ťapajna, L. Válik, F. Gucmann, D. Gregušová, K. Frohlich, Š. Haščík, E. Dobročka, L. Tóth, B. Pécz, and J. Kuzmík, J. Vac. Sci. Technol. B **35**, 01A107 (2017).
[33]G. Dutta, S. Turuvekere, N. Karumuri, N. DasGupta, and A. DasGupta, IEEE Electron Device Lett. **35**, 1085 (2014).
[34]M. Blaho, D. Gregušová, Š. Haščík, M. Jurkovič, M. Ťapajna, K. Fröhlich, J. Dérer, J. F. Carlin, N. Grandjean, and J. Kuzmík, Phys. Status Solidi A **212**, 1086 (2015).
[35]C. Mahata, S. Mallik, T. Das, C. K. Maiti, G. K. Dalapati, C. C. Tan, C. K. Chia, H. Gao, M. K. Kumar, S. Y. Chiam, H. R. Tan, H. L. Seng, D. Z. Chi, and E. Miranda, Appl. Phys. Lett. **100**, 062905 (2012).
[36]E. Miranda, J. Suñé, T. Das, C. Mahata, and C. K. Maiti, J. Appl. Phys. **112**, 064113 (2012).
[37]T. Ui, M. Kudo, and T. Suzuki, Phys. Status Solidi C **10**, 1417 (2013).
[38]F. Bernardini, V. Fiorentini, and D. Vanderbilt, Phys. Rev. B **63**, 193201 (2001).
[39]O. Ambacher, B. Foutz, J. Smart, J. R. Shealy, N. G. Weimann, K. Chu, M. Murphy, A. J. Sierakowski, W. J. Schaff, L. F. Eastman, R. Dimitrov, A. Mitchell, and M. Stutzmann, J. Appl. Phys. **87**, 334 (2000).
[40]J. A. Garrido, J. L. Sanchez-Rojas, A. Jimenez, E. Munoz, F. Omnes, and P. Gibart, Appl. Phys. Lett. **75**, 2407 (1999).
[41]E. J. Miller, E. T. Yu, C. Poblenz, C. Elsass, and J. S. Speck, Appl. Phys. Lett. **80**, 3551 (2002).
[42]A. T. Winzer, R. Goldhahn, G. Gobsch, A. Link, M. Eickhoff, U. Rossow, and A. Hangleiter, Appl. Phys. Lett. **86**, 181912 (2005).
[43]G. L. Snider, *Computer Program 1D Poisson/Schrödinger: A Band Diagram Calculator* (University of Notre Dame, Notre Dame, Indiana, 1995).
[44]E. H. Nicollian and J. R. Brews, *MOS (Metal Oxide Semiconductor) Physics and Technology* (Wiley-Interscience, Hoboken, New Jersey, 1982).
[45]E. J. Miller, X. Z. Dang, H. H. Wieder, P. M. Asbeck, E. T. Yu, G. J. Sullivan, and J. M. Redwing, J. Appl. Phys. **87**, 8070 (2000).
[46]B. Gaffey, L. J. Guido, X. W. Wang, and T. P. Ma, IEEE Trans. Electron Devices **48**, 458 (2001).
[47]R. Stoklas, D. Gregušová, J. Novák, A. Vescan, and P. Kordoš, Appl. Phys. Lett. **93**, 124103 (2008).
[48]M. Miczek, C. Mizue, T. Hashizume, and B. Adamowicz, J. Appl. Phys. **103**, 104510 (2008).
[49]J. J. Freedsman, T. Kubo, and T. Egawa, Appl. Phys. Lett. **99**, 033504 (2011).
[50]X.-H. Ma, J.-J. Zhu, X.-Y. Liao, T. Yue, W.-W. Chen, and Y. Hao, Appl. Phys. Lett. **103**, 033510 (2013).
[51]Y. Hori, Z. Yatabe, and T. Hashizume, J. Appl. Phys. **114**, 244503 (2013).
[52]K. Lehovec, Appl. Phys. Lett. **8**, 48 (1966).